Radiation induced cytochrome c release causes loss of rat colonic fluid absorption by damage to crypts and pericryptal myofibroblasts

J R Thiagarajah, P Gourmelon, N M Griffiths, F Lebrun, R J Naftalin, K C Pedley

Abstract

***Background*—Therapeutic or accidental exposure to radiation commonly causes gastrointestinal disturbances, including diarrhoea. Rats subjected to whole body ionising radiation at a dose of 8 Gy lose their capacity to absorb fluid via the descending colon after four days. After seven days, fluid absorption recovers to control levels.**

***Aims*—To investigate the effect of ionising radiation on colonic permeability together with its effect on mitochondria dependent apoptotic signals and intercellular adhesion molecules.**

***Methods*—Rats were irradiated with doses of 0–12 Gy. Colonic permeability was measured by accumulation of fluorescein isothiocyanate (FITC) dextran in crypt lumens. Changes in levels of cytochrome c, caspase 3, E and OB cadherin, β-catenin smooth muscle actin, and collagen IV were assessed using immunocytochemistry with confocal microscopy.**

***Results*—Cytosolic cytochrome c increased after 8 Gy ($t_{1/2}$ 1.4 (0.6) hours) and peaked at approximately six hours. Caspase 3 increased more slowly, particularly in crypt epithelial cells ($t_{1/2}$ 57 (14.5) hours). Pericryptal myofibroblasts disintegrated within 24 hours as was evident from loss of OB cadherin and smooth muscle actin. This coincided with increased crypt permeability to dextran. Intercellular adhesion between crypt luminal cells was not lost until day 4 when both β-catenin and E-cadherin were minimal. The half maximal dose-response for these effects was in the range 2–4 Gy. Recovery of colonic transport was concurrent with recovery of pericryptal smooth muscle actin and OB cadherin. The pan caspase inhibitor Z-Val-Ala-Asp.fluoromethylketone (1 mg/kg per day) had a small effect in conserving the pericryptal sheath myofibroblasts and sheath permeability but had no systemic therapeutic effects.**

***Conclusions*—These data suggest that radiation damage to the colon may be initiated by mitochondrial events. Loss of crypt fluid absorption and increased permeability coincided with decreased intercellular adhesion between crypt epithelial cells and loss of pericryptal sheath barrier function.**

(*Gut* 2000;**47**:675–684)

Keywords: colon; cytochrome c; myofibroblast; pericryptal sheath; cadherin; radiation

Institut de Protection et de Sûreté Nucléaire, Fontenay aux Roses, France
J R Thiagarajah
P Gourmelon
N M Griffiths
F Lebrun

King's College London, Guy's Campus, London, UK
J R Thiagarajah
R J Naftalin
K C Pedley

Correspondence to:
R J Naftalin, Kings College London, Guys Campus, New Hunts House, Rm 2–32, London Bridge, London SE1 1UL, UK.
richard.naftalin@kcl.ac.uk

Accepted for publication
23 May 2000

Previous studies have demonstrated that 3–4 days after whole body irradiation at 8 Gy, fluid absorption in the rat descending colon in vivo is impaired by 80–90%.[1] Radiation induced damage to the colon is important as loss of absorptive capacity may result in failure of the colon to compensate for radiation induced decreases in fluid absorption in the small intestine. The colon is vulnerable to ionising radiation, particularly during pelvic irradiation. Moreover, the severity of colonic damage has been suggested as an indicator of survival following total body irradiation (TBI).[2] As with the small intestine, renewal of the colonic mucosa depends on stem cell survival which is very sensitive to radiation damage. However, the myofibroblasts of the pericryptal sheath, which have an important role in colonic fluid absorption, have also been shown to be sensitive to ionising radiation.[3 4]

The ability of the large intestine to consolidate faeces is primarily dependent on the capacity of distal colonic crypts to absorb fluid against the high hydraulic resistance imposed by faeces.[5 6] Production of the necessary suction tension is dependent on the capacity of the crypts to generate a hypertonic NaCl absorbate. NaCl absorbed by crypt epithelial cells is trapped in the pericryptal space by a sheath layer surrounding the descending colonic crypts. This barrier retards Na^+ movement from the pericryptal space into the submucosa and pericryptal capillaries, thereby permitting a large osmotic gradient to be produced across the crypt walls. This induces net fluid outflow across the crypt walls, which in turn leads to suction of fluid from faeces as fluid tension is developed in the crypt lumen.[7]

The pericryptal sheath consists of a network of myofibroblast cells and extracellular matrix immediately subjacent to the crypt epithelium.[8–10] The sheath cells are held together predominantly by adherens junctions which consist of cadherins attached to the underlying actin cytoskeleton via β-catenin.[11 12] Crypt epithelial cells are also held together by adherens junctions, and tight and desmosomal junctions.[13] Pericryptal sheath function is up- or downregulated by low or high Na^+ diets,

Abbreviations used in this paper: TBI, total body irradiation; Z-vad-FMK, Z-Val-Ala-Asp. fluoromethylketone; PBS, phosphate buffered saline; FITC, fluorescein isothiocyanate.

respectively, and this correlates with colonic mucosal absorptive capacity.[14] Na^+ depletion upregulates aldosterone and angiotensin II secretion which are also trophic stimulants of myofibroblasts in wound tissue.[15]

Cytotoxic/genotoxic insults such as ionising radiation have been shown to induce apoptotic responses in a variety of cells.[16] One of the main signals in the apoptotic cascade is mitochondrial release of cytochrome c, which results in activation of the CED/ICE family of proteases, the caspases.[17] This induces proteolysis of β-catenin and subsequent loss of E-cadherin from the plasma membrane.[18] When intercellular connections are severed, the isolated colonocytes undergo rapid apoptosis.[19] It has also been suggested that cells of the pericryptal sheath detach from the basal lamina after ionising radiation exposure.[4]

One possible method of intervention in the apoptotic signalling pathway is the use of caspase inhibitors. One such inhibitor, Z-Val-Ala-Asp.fluoromethylketone (Z-vad-FMK), is a pan caspase inhibitor which has been shown to prevent apoptosis in cells[20] and has also been shown to attenuate ischaemic injury and tumour necrosis factor induced apoptosis in treated animals.[21 22]

In this study, we show that the reduced capacity of irradiated colonic crypts to absorb fluid coincides with loss of pericryptal sheath integrity and cell adhesion within crypts. This is preceded by release of cytochrome c in the period immediately following irradiation. This leads to dose related increases in caspase 3 and decreases in β-catenin, smooth muscle actin, and OB and E-cadherin.

Materials and methods

IRRADIATION PROCEDURE

Experiments were performed on male Wistar rats (315–360 g) obtained from CERJ (LeGenest, St Isle, France) which were housed, four per cage, and kept under constant temperature (21°C) with a 12:12 light-dark cycle. Rats had free access to food (normal rat chow; 105UAR, France) and water throughout the experimental period. During irradiation, rats were conscious and restrained through a ventilated plexiglass tube placed perpendicular to the beam axis and then turned on the horizontal axis to receive homogeneous whole body radiation. Animals were irradiated using a ^{60}Co source at various doses of 2–12 Gy at a dose rate of 1 Gy/min. Control animals were treated in exactly the same manner but not exposed to the source (sham irradiation) and all were treated at the same time of day.

Animals were killed by cervical dislocation at several time points (one, six, 12, and 24 hours, and two, four, seven, and 11 days) after exposure to sham and radiation sources. The distal and proximal colon was removed rapidly and the contents removed by washing with buffer. Colonic mucosa was stripped of its muscle layer and fixed in 2% paraformaldehyde in phosphate buffered saline (PBS) at 37°C for 30 minutes. The tissue was washed and stored in PBS at 4°C.

CONFOCAL MICROSCOPY

The tissue was viewed using a Nikon Diaphot inverted microscope with Nikon Fluor 20× and 60× lenses. The microscope was attached to an MRC 600 confocal scanhead, equipped with two detection channels and an Ar/Kr mixed gas laser allowing excitation at 488 nm and 568 nm. Z axis movement, with 0.1 μm resolution, was provided by a software controlled stepper motor attached to the fine focus control.

ACCUMULATION OF FITC DEXTRAN IN CRYPTS FROM ISOLATED MUCOSA

Fluorescein isothiocyanate (FITC) labelled dextran (molecular weight 10 000, FITC dextran; Sigma Chemicals, St Louis, Missouri, USA) enters and accumulates in colonic crypt lumens as a result of fluid extraction due to the osmotic gradient across the crypt wall. This leads to concentration polarisation of the macromolecular dye within the lumen. The extent of concentration polarisation is a measure of the rate of fluid absorption by the crypts.[6 7]

The procedures performed were as described by Naftalin and colleagues.[7] Colonic mucosa was stripped of its muscle layer and mounted as a 5 mm^2 sheet in a temperature controlled perfusion chamber at 35°C. The perfusion chamber was perfused with modified Tyrode (mM: NaCl 136.9; KCl 4.0; $CaCl_2$ 1.8; $NaHCO_3$ 11.8; NaH_2PO_4 0.9; Na formate 4.3; glucose 5.6). Total measured osmolality of the Tyrode solution was 289 mmol/kg. The solution prior to perfusion was gassed with 95% O_2:5% CO_2 to maintain pH 7.3–7.4.

Perfusion media were continuously passed over the tissues via a prewarming loop and a pair of back to back solenoid valves (Lee Products Ltd, Gerrards Cross, UK) which enabled the solutions to be maintained at 35±0.1°C and changed in less than one second. Medium was aspirated at the opposite side of the chamber using a suction micropipette and resulted in a near laminar flow of medium.

ESTIMATION OF THE AVERAGE CONCENTRATION OF DEXTRAN FITC IN CRYPT LUMEN

Crypt luminal and pericryptal concentration of FITC dextran was estimated by monitoring the ratio of fluorescence intensity of the dye in the crypt lumen at any depth, x, to that in the crypt luminal opening, x=0. The relative changes in luminal concentrations of FITC dextran were quantified using fluorescence after attenuation of the signal with a neutral density filter (3% transmittance) and subtraction of background. With this high level of neutral density filtration there is no detectable autofluorescence from the tissue.

The ratio $(I_x-I_{bkg})/(I_{co}-I_{bkg})$ in the crypt lumen is equivalent to the concentration polarisation at varied depths x (where I_x is the fluorescence intensity in the crypt lumen at a distance x from the crypt luminal opening, I_{co}; and I_{bkg} is fluorescence in the absence of dye; I_{bkg}=30–50 units/pixel). Estimates of average fluorescence intensity in the crypt lumen were obtained by taking the pixel intensity of circumscribed areas of interest within 6–8 crypt lumens, 500–1000 pixels per area. The

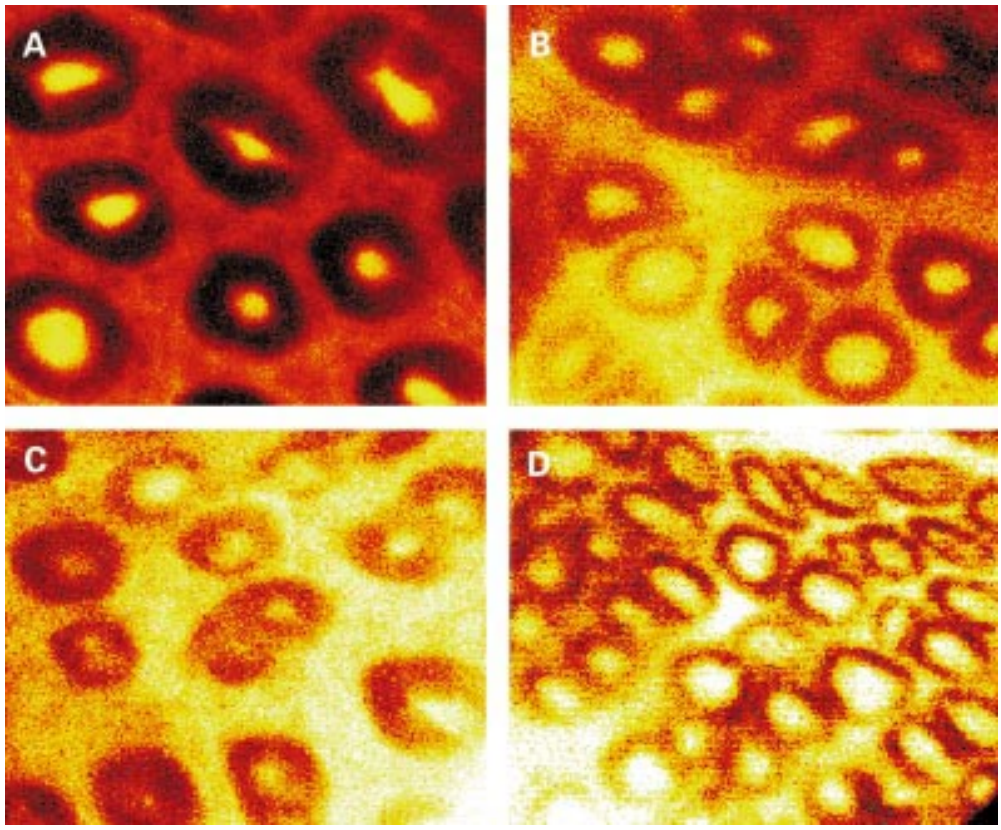

Figure 1 Confocal images at a depth of 40 μm from the luminal surface. (A) Control rats accumulate dextran within crypt lumens 10 times above that in external solution. Two (B) and four (C) days after radiation (8 Gy), reduced accumulation in crypt and increased leakage into the pericryptal region are seen. Seven days after irradiation (D) some recovery with increased accumulation in crypt lumens is evident.

maximum pixel light intensity was 256 units background. The intensities of the same regions in the crypt lumen at successive depths were computed.

IMMUNOCYTOCHEMISTRY

Staining procedure

Colonic mucosal tissue (0.5 cm^2 pieces) was placed in 1.5 ml Eppendorf tubes. The tissue was stained according to the following protocol. The procedure was the same for all antibodies used. The tissue was permeabilised in 0.2% Triton X-100 in PBS for 30 minutes, washed twice in PBS, and incubated in blocking buffer (2% goat serum in PBS or 5% fetal calf serum) for 30 minutes. The tissue was then incubated for 60 minutes with primary antibody (1:100), washed 3× in blocking buffer, and incubated for 60 minutes in each secondary antibody (1:100) and left in blocking buffer.

Antibodies

Antibodies were obtained from the following agencies: RDI goat anti-CPP32 p20 C-Term (Hu/Ms/Rt) (caspase 3), RDI goat anticatenin-β C-Term (Hu/Ms/Rt), RDI goat anticadherin-E (Hu/Ms/Rt), RDI mouse anticytochrome c clone 6H2.B4, Santa Cruz Goat anti-OB cadherin (C-16), Sigma monoclonal anti-α smooth muscle actin clone IA4, and RDI rabbit anticollagen type IV. For anticaspase 3, anticadherin-E, and anti-OB cadherin stained tissue, biotin antigoat IgG was used as the secondary antibody followed by Alexa-488 NeutrAvidin; for anticytochrome C and anti-α smooth muscle actin staining, Texas Red goat antimouse IgG was used. All secondary antibodies and Alexa-488 were supplied by Molecular Probes, Eugene, Oregon, USA.

CONFOCAL IMAGES

Each piece of tissue was taken and viewed under the confocal microscope using a Nikon 60×/1.4na Plan Apochromat oil immersion lens. The tissue was viewed from the mucosal side. The focus plane was taken to the surface of the tissue and images were captured at 10 μm steps using the automatic Z step motor. Images were taken from 0 μm to 40 μm below the surface. Images represented as much as possible the general level of staining throughout the whole tissue.

IMAGE ANALYSIS

The captured images were analysed using the public domain NIH image program (written by Wayne Rasband at the US National Institutes of Health) to quantify the fluorescence from each antibody. Fluorescence was evaluated by measuring mean fluorescence intensity of a designated region from either the crypt or the intercryptal space, at each of five focal planes. Three areas of both crypt and intercrypt were taken per image, giving 30 measurements per tissue at the different depths. Also, one area per image was taken as a background value.

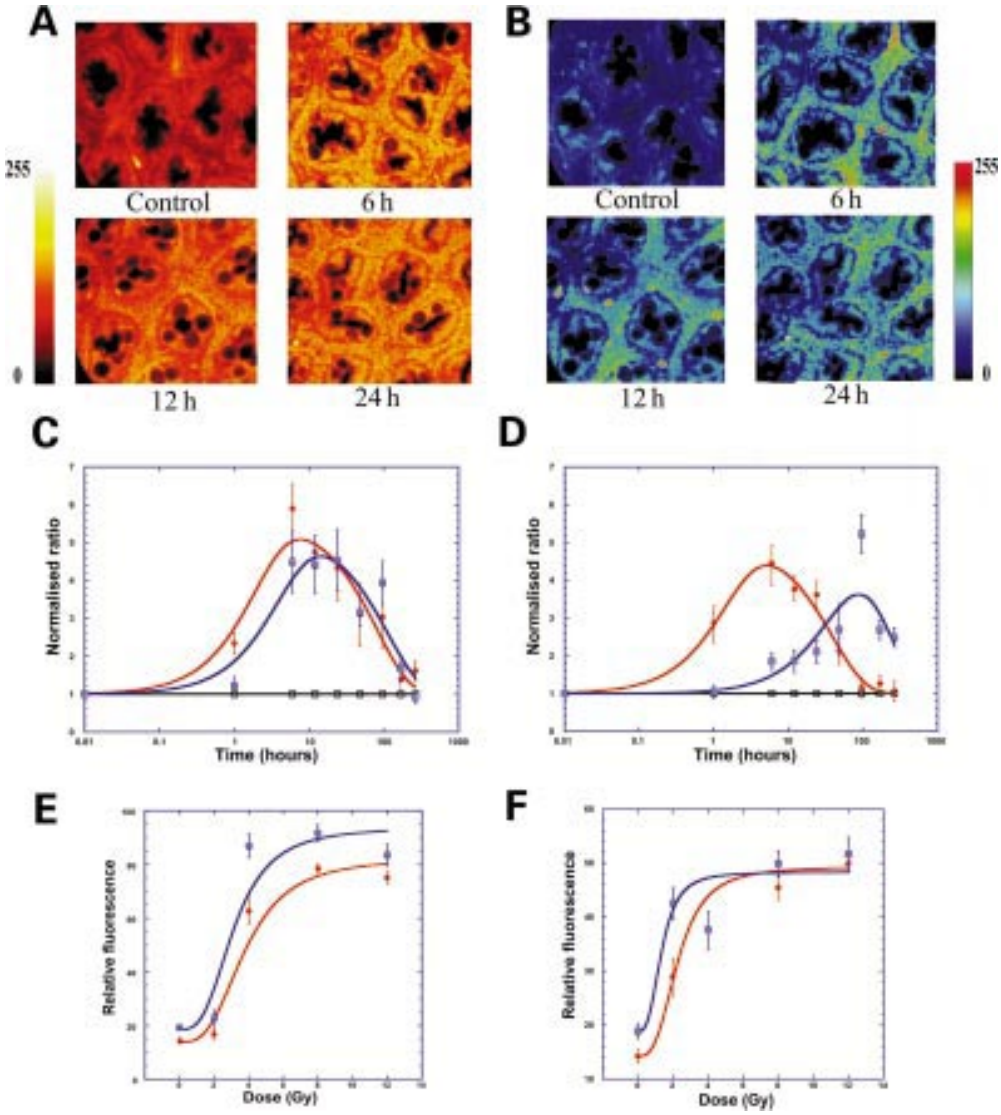

Figure 2 Rapid release of cytochrome c after radiation in both crypt and pericrypt regions and appearance of caspase 3. (A) Confocal images (depth 20 μm) showing cytochrome c after 8 Gy radiation in rat colon in controls and after six, 12, and 24 hours. (B) Confocal images (depth 20 μm) showing caspase 3 after 8 Gy radiation in rat colon in controls and after six, 12, and 24 hours. (C) Time course of cytochrome c (red) and caspase 3 (blue) in pericryptal sheath after 8 Gy radiation showing a small time lag between maximal increases. Data shown (n=3) as normalised ratios on a log scale against controls taken from the pericryptal region. Cytochrome c data were plotted with a biphasic exponential fit giving half times for the increase and decrease (see table 1 and materials and methods). (D) Time course of cytochrome c (red) and caspase 3 (blue) in crypt cells after 8 Gy radiation showing a large time lag between maximal increases. Data from crypt regions of same images used for (C). (E) Dose-response (0–12 Gy) curve for cytochrome c release after 12 hours in pericryptal (red) and crypt (blue) cells. Data shown as relative fluorescence (n=3) plotted with a non-linear Michaelis-Menten curve fit showing a saturable dose-response. (F) Dose-response (0–12 Gy) curve for caspase 3 after 12 hours in pericryptal (red) and crypt (blue) cells. Data shown as relative fluorescence (n=3) plotted with a non-linear Michaelis-Menten curve fit showing a saturable dose-response.

DATA ANALYSIS AND CURVE FITTING

Mean (SEM) measurements corrected for background from each image were calculated. The means for a particular series such as time course or dose were tabulated. Mean (SEM) numbers at two depths were then taken. For the most part this was either at 20 μm and 30 μm or at 30 μm and 40 μm, respectively. For the dose series the resultant values were plotted directly against dose. For the time course series the values at each time point were normalised relative to the control value and plotted as a ratio. For cytochrome c and caspase, data were fitted to curves with an exponential rise followed by exponential decay using the non-linear least squares curve fitting procedure incorporated into KaleidaGraph (Synergy Software). For OB cadherin and smooth muscle actin, data were fitted to curves with an exponential decay followed by an exponential rise. The equation for both was of the type: $C_{Rt}=C_{A0}k_1((e^{-k_1 t}/(k_2-k_1))+(e^{-k_2 t}/(k_1-k_2))$, where C_{Rt} is the cell density of varying substance at time t, C_{AO} is a scale factor, and k_1 and k_2 are the first and second exponential rates.

CASPASE INHIBITOR TREATMENT

Rats were irradiated as previously at a dose of 8 Gy. Immediately after irradiation the animals were treated with the caspase inhibitor Z-vad-FMK (purchased from Calbiochem) 1 mg/kg by intraperitoneal injection per day. Animals were treated every day for three days and then killed on day four. Tissue for dextran

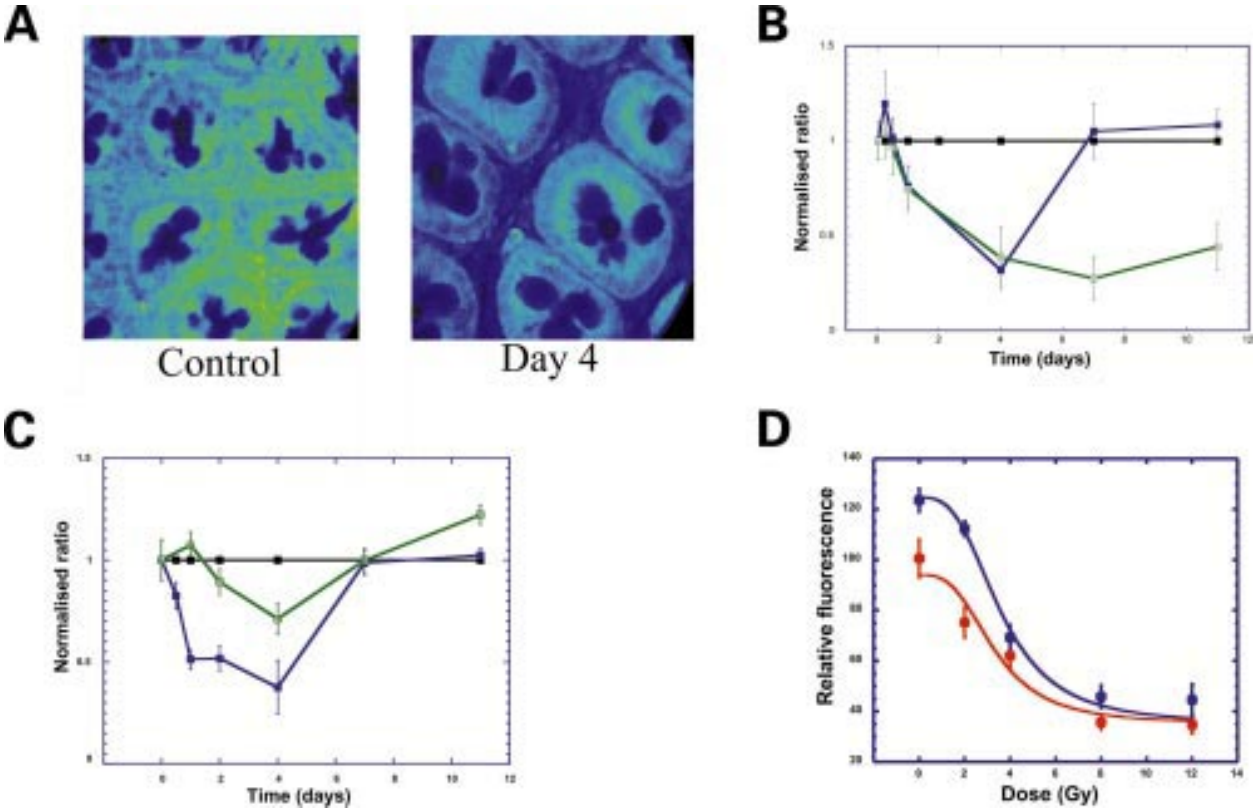

Figure 3 Decrease in E-cadherin and β-catenin in colon 2–4 days after radiation. (A) Confocal images (depth 20 μm) showing decrease in E-cadherin four days after radiation, particularly in the pericryptal region. (B) Time course of E-cadherin in pericryptal (blue) and crypt (green) cells after 8 Gy radiation showing a decrease in both the pericrypt and crypt and recovery in pericryptal cells. Data shown (n=3) as normalised ratios against control. (C) Time course of β-catenin in pericryptal (blue) and crypt (green) cells after 8 Gy radiation showing a decrease in both the pericrypt and crypt and recovery in both pericryptal and crypt cells. Data shown (n=3) as normalised ratios against control. (D) Dose-response of E-cadherin (0–12 Gy) showing a saturable decrease. Data shown as relative fluorescence (n=3) and plotted using a non-linear Michaelis-Menten fit.

accumulation and immunocytochemistry was collected as before.

Results

LOSS OF ABILITY TO CONCENTRATE FITC DEXTRAN IN CRYPTS

In the descending colon obtained from control animals, crypts accumulated dextran within their lumens at concentrations 10 times greater than at the crypt opening (fig 1). However, following TBI (8 Gy), during the two and four day post-irradiation period, the crypts only concentrated dextran by 1.5-fold. This radiation induced decrease in dextran accumulation implied at least an 85% loss in crypt absorptive power.[23] This loss was accompanied by very large increases in dextran leakage from the mucosal bathing solution into the surrounding pericryptal spaces. There are two ways that the dye can pass into the submucosal space, either via the crypt luminal wall or through the surface mucosa. It is evident that irradiation damage increased dextran permeability via both of these routes. After seven days, some recovery was evident, as accumulation of dextran into crypt lumens was increased. However, significant leakage of FITC dextran into the pericryptal space remained, as evident from the low ratio of dextran accumulation between the crypt lumen and pericryptal space.

RELEASE OF CYTOCHROME C AND APPEARANCE OF CASPASE 3 FOLLOWING RADIATION

Increases in cytochrome c were observed within one hour following 8 Gy TBI in both

Table 1 First and second rate constants (Tau K_1 and K_2, respectively) for all proteins followed from a biphasic exponential fit of the data in pericrypt and crypt regions (see materials and methods). Gy_{50} values were calculated from dose-response curves

	Tau 1/K_1 (h) Rate of appearance		*Tau 1/K_2 (h) Rate of loss*		*Gy_{50}*	
	Pericrypt	*Crypt*	*Pericrypt*	*Crypt*	*Pericrypt*	*Crypt*
Cytochrome c	2.0 (0.8)	1.4 (0.2)	83.3 (20.8)	40.0 (4.8)	3.8 (0.3)	3.2 (0.2)
Caspase	7.7 (3.0)	16.7 (5.6)	76.9 (17.7)	166.7 (83.4)	2.3 (0.3)	1.4 (0.3)
	Tau 1/K_1 (h) Rate of loss		*Tau 1/K_1 (h) Rate of recovery*		*Gy_{50}*	
	Pericrypt	*Crypt*	*Pericrypt*	*Crypt*	*Pericrypt*	*Crypt*
OB cadherin	5.0(2.8)	—	58.8 (27.7)	—	1.3 (0.2)	—
SM actin	16.7(5.6)	—	66.7 (22.2)	—	2.9 (0.5)	—
β-catenin	26.3(13.8)	50.0 (15.8)	—	—	1.6 (0.1)	1.8 (0.4)
E-cadherin	66.6(24.8)	83.3 (64.1)	—	—	3.3 (0.4)	3.4 (0.3)

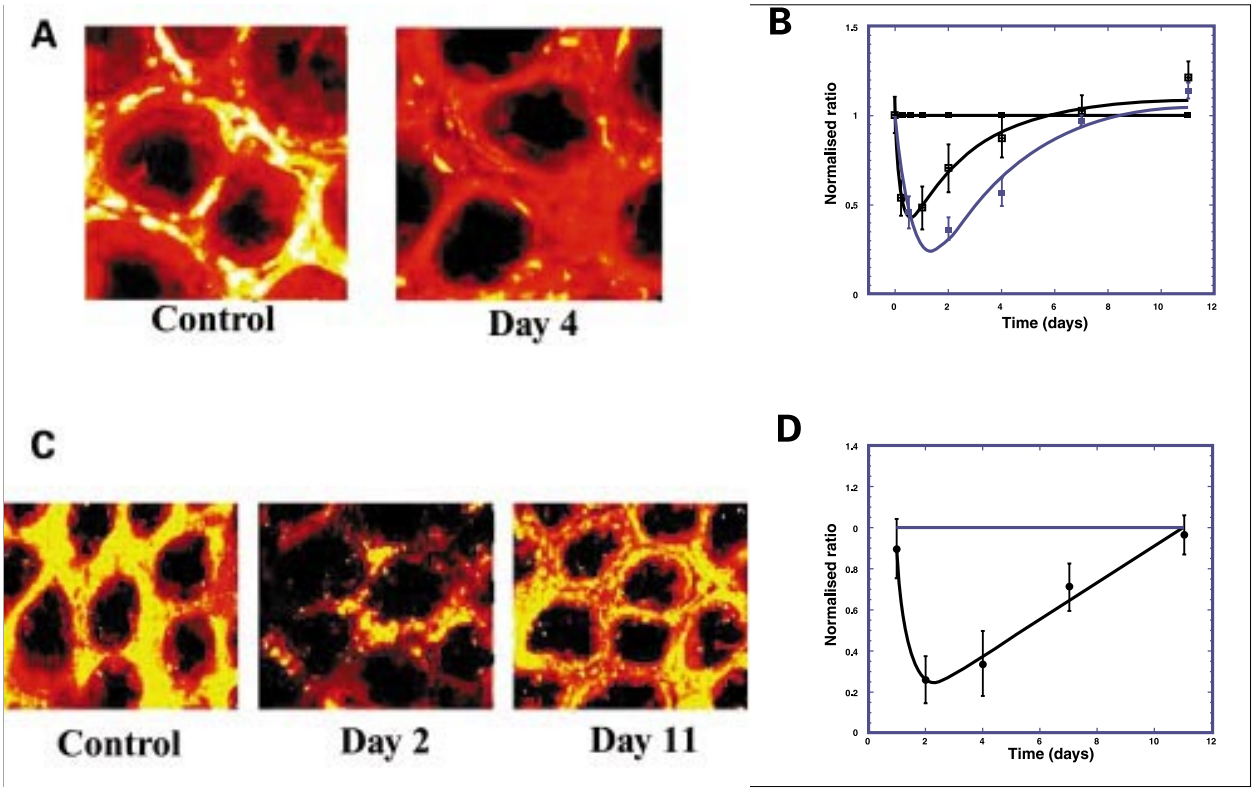

Figure 4 Decrease in α smooth muscle actin, OB cadherin, and collagen type IV in pericryptal sheath region after radiation. (A) Confocal images (depth 20 μm) showing decrease in smooth muscle actin in pericryptal areas after 8 Gy radiation. (B) Time course of smooth muscle actin (blue) and OB cadherin (green) in pericryptal sheath cells after 8 Gy radiation showing maximal decreases at two days and recovery after seven days. Data shown (n=3) as normalised ratios against control. (C) Confocal images (depth 20 μm) showing decrease in collagen type IV in pericryptal areas after 8 Gy radiation. (D) Time course of collagen type IV in pericryptal sheath after 8 Gy radiation showing maximal decreases at 2–4 days and recovery after 11 days. Data shown (n=3) as normalised ratios against control.

crypt and pericryptal cells. In the intercrypt region, which contains the pericryptal myofibroblastic sheath, the $t_{1/2}$ of the increase in cytochrome c was 1.4 (0.6) hours and peaked at about six hours. This was followed by an exponential decrease in cytochrome c with a $t_{1/2}$ of 57.8 (14.5) hours. At 11 days, cytochrome c had almost returned to control levels. A similar progression was seen in the crypt epithelial cells with a $t_{1/2}$ of 1.1 (0.2) hours for the increase and 27.7 (3.3) hours for the decrease. The half times were calculated from a biphasic exponential fit of these time courses (fig 2C, D). Staining of anticytochrome c antibody in colonic mucosa from controls and irradiated animals (at six, 12, and 24 hours) is shown in the images in fig 2A.

Cytochrome c release into the cytosol observed 12 hours after radiation increased as a saturable function of radiation dose both in the crypt epithelial cells and in the cells of the pericryptal sheath (fig 2E). The half maximal response of both types of cell was 2–4 Gy. The monoexponential time course of cytochrome c appearance suggested that the release came from a single uniformly radiosensitive source, namely the mitochondria.

The increase in caspase 3 following radiation was, in common with cytochrome c, biphasic: a rapid increase followed by a slow decrease (fig 2C, D). However, the initial rise in caspase 3 in the pericryptal myofibroblasts was slower ($t_{1/2}$ 2.9 (1.6) hours) than that of cytochrome c. In the crypt epithelial cells the increase in caspase was much slower than that of cytochrome c, with a $t_{1/2}$ of 11.5 hours and levels remaining high at four days (fig 2D).

There was also a saturable relationship between caspase 3 activation and radiation dose in the crypt epithelial cells and in the pericryptal myofibroblasts at 12 hours, with a half maximal response at 1–3 Gy (fig 2F). In both crypt and pericrypt regions the response to radiation had a threshold of 1–2 Gy. Only minimal release of cytochrome c and caspase was observed below this radiation level. Little additional release was seen on raising the radiation dose from 8 to 12 Gy. The significant delay in the appearance of caspase 3 after cytochrome c indicated that caspase activation occurred 2–3 hours after the rise in cytochrome c. The much slower rate of decrease in caspase 3 than that of cytochrome c was consistent with continuous generation of caspase, which may have been stimulated by low levels of cytochrome c remaining in the cytosol.

LOSS OF E-CADHERIN AND β-CATENIN

The increased macromolecular leakage through wide paracellular channels in the crypt walls after radiation suggested loss of the cell adhesion molecules. To test this hypothesis, levels of the cell adhesion molecules E-cadherin and β-catenin were quantified following radiation exposure.

After radiation, E-cadherin was reduced (fig 3A, B) in the pericryptal regions within two days and in the crypts at four days. After seven

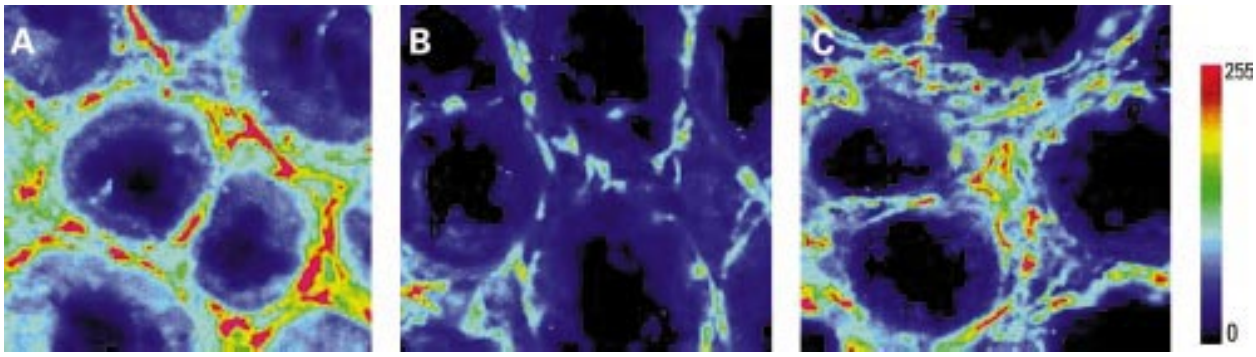

Figure 5 Effect of Z-vad-FMK treatment on α smooth muscle actin in the pericryptal sheath region after radiation. Confocal images (depth 20 μm) showing (A) control, (B) irradiated (8 Gy)+vehicle treated, and (C) irradiated (8 Gy)+Z-vad-FMK treated.

days some recovery in E-cadherin was evident in the pericryptal region but not in the crypts. The response of E-cadherin loss at two days to radiation dose (fig 3D) showed a saturable response, which was half maximal at 2–4 Gy.

β-Catenin was also reduced after radiation with maximal loss at 2–4 days (fig 3C). Greater loss was evident in the pericryptal than in the crypt luminal cells. Levels of β-catenin recovered both in the pericrypt and crypt at seven and 11 days after radiation. At two days β-catenin had a similar saturable inhibitory response to radiation as E-cadherin, with a similar half maximal response at 1–3 Gy (table 1).

LOSS AND RECOVERY OF OB CADHERIN, α SMOOTH MUSCLE ACTIN AND COLLAGEN TYPE IV

OB cadherin (cadherin 11) is an adhesion molecule specific to mesenchymal cells such as myofibroblasts and macrophages.[24 25] After radiation, OB cadherin levels decreased rapidly with maximal loss at 24 hours ($t_{1/2}$ 3.5 (2) hours) and recovery after seven days (fig 4B). The rapid loss in OB cadherin in the pericryptal region shows that myofibroblasts were particularly sensitive to radiation. This was confirmed by the higher radiation sensitivity of OB cadherin loss (Gy_{50} <2Gy) compared with E-cadherin.

Smooth muscle actin is a marker of myofibroblasts in the pericryptal sheath as well as in wound tissue.[10 26] In common with OB cadherin, it too is very radiosensitive. After radiation there was a maximal decrease in smooth muscle at 2–4 days indicating loss of the pericryptal myofibroblasts within this time frame. The radiation dose-response of this antigen was similar to that of OB cadherin (Gy_{50} 1–3 Gy). Recovery of smooth muscle actin in the pericryptal region, similar to OB cadherin, was rapid. After seven days levels returned to control values and increased above control at 7–11 days (fig 4A, B).

Collagen type IV is one of the main matrix constituents of the pericryptal sheath and basement membrane and is produced by the pericryptal myofibroblasts.[27] As with smooth muscle actin and OB cadherin, it is lost rapidly after radiation and then recovers (fig 4C, D).

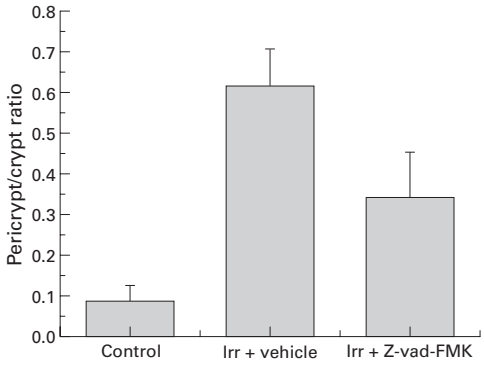

Figure 6 Effect of Z-vad-FMK treatment on FITC dextran accumulation after radiation. Ratio of pericrypt to crypt fluorescence in control, irradiated (irr) (8 Gy)+vehicle treated, and irradiated (8 Gy)+Z-vad-FMK treated.

EFFECTS OF CASPASE INHIBITOR Z-vad-fmk TREATMENT ON COLONIC PERMEABILITY AND PERICRYPTAL SHEATH INTEGRITY

There was no evidence that the caspase inhibitor Z-vad-fmk had any favourable effect on weight loss, neutropenia, or loss of thymus weight following radiation. Furthermore, there was no significant effect of Z-vad-fmk on net fluid absorption from treatment than in irradiated but untreated animals in the descending colon in vivo, four days after irradiation with 8 Gy. However, after treatment with Z-vad-fmk there was some evidence of protection of the pericryptal sheath (fig 5). There was more smooth muscle actin after treatment, indicating the increased presence of myofibroblasts in the sheath. However, the pattern of staining showed the myofibroblasts to be only loosely associated with the crypts unlike the connected sheath structure seen in controls. These observations were borne out by the effect of Z-vad-fmk on dextran accumulation (fig 6) which showed some decrease in leakage into the pericryptal space compared with untreated but irradiated animals. However, this effect was significant only at the one tailed level ($p<0.037$).

Discussion

The rapidity of the monoexponential release of cytochrome c from mitochondria, and the saturable response to radiation dose in both crypt epithelial and pericrypt myofibroblasts, indicates that it is triggered by one or a combination of factors in the period during and immediately following radiation (for example, production of radiation induced free radicals, release of ceramide from radiation induced membrane sphingomyelin breakdown,[28] or

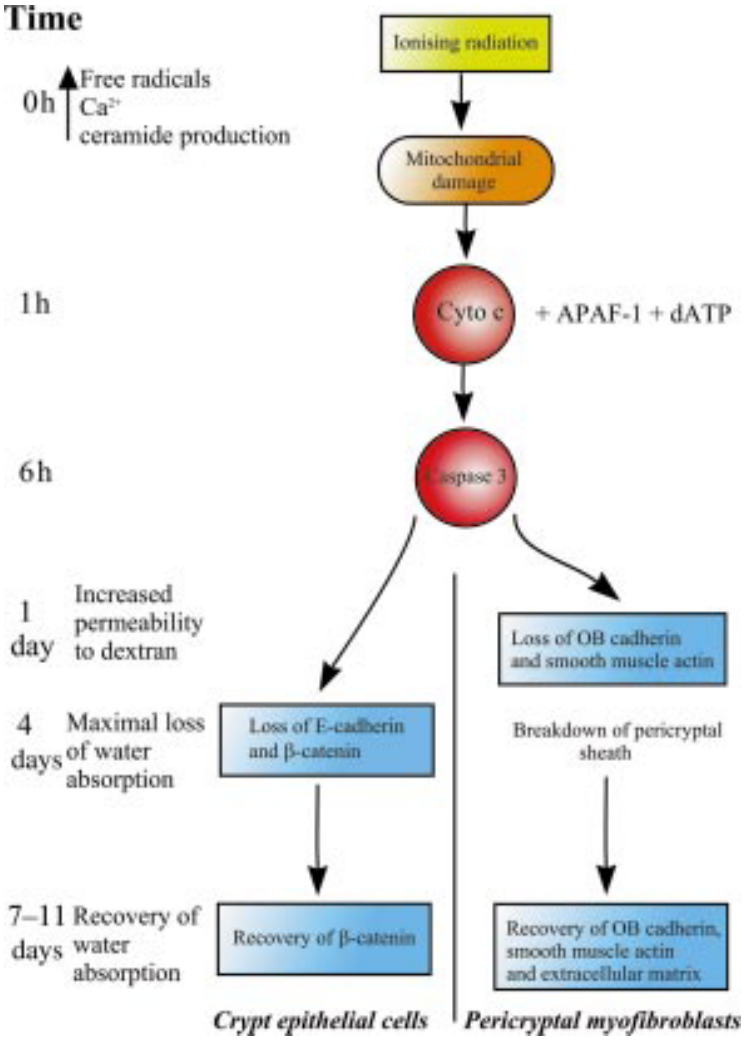

Figure 7 Summary diagram showing possible pathway after radiation in the colon and relationship to functional changes.

increases in cell death signalling proteins) (fig 7).[29] The method of cytochrome c release remains controversial and may be related to depolarisation of the mitochondrial membrane[30] and/or the formation of pores by pro-apoptotic proteins such as Bad, Bak, Bid, and Bax. Recent evidence suggests that cytochrome c release can occur while the mitochondrial membrane potential is maintained.[31] In fact, in experiments carried out in human leukaemic cells (MOLT-4), exposure to 5 Gy gamma radiation resulted in loss of mitochondrial membrane potential followed by increased caspase 3 levels.[32]

INITIAL RESPONSE TO RADIATION

Myofibroblasts have both faster caspase activation and higher radiosensitivity than crypt epithelial cells. This suggests that the relative sensitivities of different cell types may be related to the sensitivity of caspase activation to cytoplasmic cytochrome c concentration. It is evident that while cytochrome c release rates are similar in the pericryptal and crypt epithelial cells, the downstream process activated by cytochrome c release is slower in crypt epithelial cells than in the pericryptal myofibroblasts. This suggests that caspase 3 in myofibroblasts is activated by lower concentrations of cytosolic cytochrome c than in crypt epithelial cells, and provides a basis for the variability of cell sensitivity to ionising radiation. Another possibility is the increased presence of protective substances in the crypt epithelial cells such as Bcl-2 which has been shown to delay caspase activation after cytochrome c release[33 34] and has been suggested to alter the sensitivity of caspase activation to cytochrome c.

The longer time required for caspase 3 concentrations to return to control levels compared with cytochrome c suggests that caspase 3 is continuously generated by low cytochrome c in combination with APAF-1, caspase 9, and dATP.[35] Alternatively, it may be that caspase 3 levels remain elevated through the action of other caspases by a positive feedback mechanism.[36]

In contrast with the *increases* observed in cytochrome c and caspase 3, E-cadherin and β-catenin are both *lost* from crypt epithelial cells and pericryptal myofibroblasts after radiation. This is in agreement with other data showing loss of cell-cell adhesion following a rise in caspase activity.[18]

OB cadherin and E-cadherin losses from pericryptal myofibroblasts occurred more rapidly and had similar time courses of loss to α smooth muscle actin, another myofibroblast specific antigen. This loss was maximal at 2–4 days, which is the time when fluid absorption is maximally inhibited[1] and when the colonic mucosa is most permeable to FITC dextran (fig 1).

These losses indicate that dissolution of the myofibroblast cells of the pericryptal sheath occurs *before* fluid transport is maximally inhibited and E-cadherin loss is maximal (table 1). The early loss of OB cadherin and smooth muscle actin coincide with the early increase in tissue permeability to dextran (fig 1). This finding indicates that even though the pericryptal sheath myofibroblasts are damaged, a residual capacity for absorption remains. However, maximal loss of absorption coincided with damage of *both* pericryptal myofibroblasts and crypt epithelial cells on day 4. Recovery of the sheath on days 7–11 was accompanied by only partial recovery in tissue permeability to dextran. This may be because complete recovery of fluid absorption occurs only when both the crypts and pericryptal sheath are impermeable.

The high sensitivity of the pericryptal sheath myofibroblasts to radiation damage has been reported in both human and murine colon.[3 4] These early findings, together with those reported here, indicate that myofibroblast loss and recovery rates may play at least as important a role as stem cells in determining *functional* responses to injury.

RECOVERY RESPONSE

All of the antigens showed complete recovery within the pericryptal cells within 4–11 days after irradiation. OB cadherin and smooth muscle actin recovered faster than β-catenin and E-cadherin. Additionally β-catenin and E-cadherin were much slower to recover in the

crypt epithelial cells than in pericryptal myofibroblasts. This suggests that the pericryptal sheath myofibroblasts, although easily damaged by radiation, may be rapidly replaced, whereas crypt epithelial cells, which sustain less overt radiation damage, are slower to recover.

There is little evidence of nuclear degeneration in crypt epithelial cells even though caspase 3 is activated and this is consistent with lack of evidence of cell damage on haematoxylin-eosin staining after radiation.[37] One possibility is that the crypt epithelial cells may resist nuclear damage from caspase induced activation of DNA fragmenting factor,[38 39] perhaps by some form of nuclear protection against caspase 3.[40]

There was histological evidence of recovery of the pericryptal myofibroblasts by day 7, coinciding with some recovery in crypt fluid absorption capacity in vivo against low resistance luminal content. Additionally, loss and recovery of collagen IV is further evidence of loss of sheath function followed by a recovery phase in response to irradiation. Nevertheless, even after 11 days the crypts remained more permeable to dextran than unirradiated controls. This suggests that some additional adhesive process must occur before there is full recovery of colonic barrier function.

It is possible that the increase in proteins seen in the crypts is not due to recovery of irradiated cells but to proliferation and migration of new cells generated from stem cells into the area. On the basis that stem cells lie near the base of the crypts[41] it might be expected that deeper lying crypt cells should show more rapid recovery than more superficial cells. However, as there was no evidence of faster recovery in deeper cells (50 μm) than superficial cells (20 μm) it would seem more likely that recovery is associated with repair processes in the irradiated cells. This does not apply to pericryptal myofibroblasts which could well migrate into the sheath from precursor cells in the adjacent lamina propria and replace those lost after radiation.

Treatment of irradiated animals with the broad spectrum caspase inhibitor Z-vad-FMK suggested a protective effect on the pericryptal myofibroblasts, although the structure of the sheath was not maintained. Leakage of dextran into the pericryptal space in irradiated animals was reduced by treatment, although this reduction was only significant on a one tailed *t* test ($p<0.037$) and the colonic mucosa still remained leaky.

Our study is the first to show a correlation between radiation damage at the molecular level and transport activity in vivo. As such it shows that while the changes in individual proteins are relatively clear cut, the effects of increases or decreases in their expression on transport processes are more ambiguous and must be interpreted in relation to functional processes. However, based on our findings we conclude that radiation damage in the colon is initiated by mitochondrial events that show both a threshold and maximal response to injury. These results open up new possibilities for therapeutic approaches to treat radiation injury.

The authors would like to thank Brigitte Ksas for expert technical assistance for the Z-VAD-fmk study.

1 Dublineau I, Ksas B, Aigueperse J, *et al*. In vivo alterations of fluid and electrolyte fluxes in rat colon by gamma irradiation *Dig Dis Sci* 1998;**43**:652–62.
2 Wilson SG. Radiation-induced gastrointestinal death in the monkey. *Am J Pathol* 1954;**35**:1233–51.
3 Wiernik G, Perrins D. Radiosensitvity of a mesenchymal tissue. The pericryptal fibroblast sheath in the human rectal mucosa. *Br J Radiol* 1975;**48**:382–9.
4 Neal JV, Potten CS. Effect of low dose ionizing radiation on the murine pericryptal fibroblast sheath: radiation damage in a mesenchymal system in vivo. *Int J Radiat Biol Relat Stud Phys Chem Med* 1981;**39**:2 175–83.
5 Pedley KC, Naftalin RJ. Evidence from fluorescence microscopy and comparative studies that rat, ovine and bovine colonic crypts are absorptive. *J Physiol (Lond)* 1993;**460**: 525–47.
6 Naftalin RJ, Zammit PS, Pedley KC. Concentration polarization of fluorescent dyes in rat descending colonic crypts: evidence of crypt fluid absorption. *J Physiol (Lond)* 1995;**487**:479–95.
7 Naftalin RJ, Zammit PS, Pedley KC. Regional differences in rat large intestinal crypt function in relation to dehydrating capacity *in vivo*. *J Physiol* 1999;**514**:201–10.
8 Pascal R, Kaye G, Lane N. Colonic pericryptal fibroblast sheath: replication, migration and cytodifferentiation of a mesenchymal cell system in adult tissue. I. Autoradiographic studies of normal rabbit colon. *Gastroenterology* 1968;**54**:835–51.
9 Desaki J, Fujiwara T, Komuro T. A cellular reticulum of fibroblast-like cells in the rat intestine—scanning and transmission electron-microscopy. *Arch Histol Jpn* 1984;**47**: 179–86.
10 Powell DW, Mifflin R, Valentich J, *et al*. Myofibroblasts. II. Intestinal subepithelial myofibroblasts. *Am J Physiol Cell Physiol* 1999;**277**:**1** C1–9.
11 Petridou S, Masur SK. Immunodetection of connexins and cadherins in corneal fibroblasts and myofibroblasts. *Invest Ophthalmol Vis Sci* 1996;**37**:**9** 1740–8.
12 Wheelock MJ, Knudsen KA. Cadherins and associated proteins. *In Vivo* 1991;**5**: 505–13.
13 Jawhari A, Pignatelli M, Farthing M. The importance of the E-cadherin-catenin complex in the maintenance of intestinal epithelial homoeostasis: more than intercellular glue? *Gut* 1997;**41**:581–4.
14 Naftalin RJ, Pedley KC. Regional crypt function in rat large intestine in relation to fluid absorption and growth of the pericryptal sheath. *J Physiol (Lond)* 1999;**514**:211–27.
15 Campbell SE, Katwa LC. Angiotensin II stimulated expression of transforming growth factor-beta1 in cardiac fibroblasts and myofibroblasts. *J Mol Cell Cardiol* 1997;**29**: 1947–58.
16 Harms-Ringdahl M, Nicotera P, Radford IR. Radiation induced apoptosis. *Mutat Res* 1996;**366**:**2** 171–9.
17 Li P, Nijhawan D, Budihardjo I, *et al*. Cytochrome c and dATP-dependent formation of Apaf-1/caspase-9 complex initiates an apoptotic protease cascade. *Cell* 1997;**91**:479–89.
18 Brancolini C, Lazarevic D, Rodriguez J, *et al*. Dismantling cell-cell contacts during apoptosis is coupled to a caspase-dependent proteolytic cleavage of beta-catenin. *J Cell Biol* 1997;**139**:759–71.
19 Lifshitz S, Schwartz B, Polak-Charcon S, *et al*. Extensive apoptotic death of rat colonic cells deprived of crypt habitat. *J Cell Physiol* 1998;**177**:3 377–86.
20 Tepper AD, de Vries E, van Blitterswijk WJ, *et al*. Ordering of ceramide formation, caspase activation, and mitochondrial changes during CD95- and DNA damage-induced apoptosis. *J Clin Invest* 1999;**103**:971–8.
21 Yaoita H, Ogawa K, Maehara K, *et al*. Attenuation of ischemia/reperfusion injury in rats by a caspase inhibitor. *Circulation* 1998;**97**:276–81.
22 Piguet PF, Vesin C, Donati Y, *et al*. TNF-induced enterocyte apoptosis and detachment in mice: induction of caspases and prevention by a caspase inhibitor, ZVAD-fmk. *Lab Invest* 1999;**79**:495–500.
23 Zammit PS, Mendizabal MV, Naftalin RJ. Effects on fluid and Na^+ flux of varying luminal hydraulic resistance in rat colon *in vivo*. *J Physiol* 1994;**447**:539–48.
24 Munro SB, Turner IM, Farookhi, *et al*. E-cadherin and OB-cadherin mRNA levels in normal human colon and colon carcinoma. *Exp Mol Pathol* 1995;**62**:118–22.
25 Masur SK, Conors RJ Jr, Cheung JK, *et al*. Matrix adhesion characteristics of corneal myofibroblasts. *Invest Ophthalmol Vis Sci* 1999;**40**:**5** 904–10.
26 Sappino AP, Schurch W, Gabbiani G. Differentiation repertoire of fibroblastic cells: expression of cytoskeletal proteins as marker of phenotype modulations. *Lab Invest* 1990;**63**: 144–61.
27 Mahida YR, Beltinger J, Makh S, *et al*. Adult human colonic subepithelial myofibroblasts express extracellular matrix proteins and cyclooxygenase-1 and -2. *Am J Physiol* 1997; **273**:G1341–8.

28 Haimovitz-Friedman A, Kan CC, Ehleiter D, *et al*. Ionizing radiation acts on cellular membranes to generate ceramide and initiate apoptosis. *J Exp Med* 1994;**180**:**2** 525–35.
29 Boesen-de Cock JG, Tepper AD, de Vries E, *et al*. Common regulation of apoptosis signaling induced by CD95 and the DNA-damaging stimuli etoposide and gamma-radiation downstream from caspase-8 activation. *J Biol Chem* 1999;**274**:14255–61.
30 Kluck RM, Bossy-Wetzel E, Green DR, *et al*. The release of cytochrome c from mitochondria: a primary site for Bcl-2 regulation of apoptosis. *Science* 1997;**275**:1132–6.
31 Goldstein JC, Waterhouse NJ, Juin P, *et al* The coordinate release of cytochrome c during apoptosis is rapid, complete and kinetically invariant. *Nat Cell Biol* 2000;**2**:156–62.
32 Zhao Q-L, Kondo T, Noda A, *et al*. Mitochondrial and intracellular-free calcium regulation of radiation-induced apoptosis in human leukemic cells. *Int J Radiat Biol* 1999; **75**:493–504.
33 Chaloupka R, Petit PX, Israel N, *et al*. Over-expression of Bcl-2 does not protect cells from hypericin photo-induced mitochondrial membrane depolarization, but delays subsequent events in the apoptotic pathway. *FEBS Lett* 1999; **462**:295–301.
34 Rosse T, Olivier R, Monney L, *et al*. Bcl-2 prolongs cell survival after Bax-induced release of cytochrome c. *Nature* 1998;**391**:496–9.
35 Zou H, Henzel WJ, Liu XS, *et al*. Apaf-1, a human protein homologous to C-elegans CED-4, participates in cytochrome c-dependent activation of caspase-3. *Cell* 1997;**90**: 405–13.
36 Van de Craen M, Declercq W, Van den brande I, *et al*. The proteolytic procaspase activation network: an in vitro analysis. *Cell Death Differ* 1999;**6**:1117–24.
37 Francois A, Dublineau I, Lebrun F, *et al*. Modified absorptive and secretory processes in the rat distal colon after neutron irradiation: in vivo and in vitro studies. *Radiat Res* 1999;**151**:468–78.
38 Kurihara H, Torigoe S, Omura M, *et al*. DNA fragmentation induced by a cytoplasmic extract from irradiated cells. *Radiat Res* 1998;**150**:**3** 269–74.
39 Mandal M, Adam L, Kumar R. Redistribution of activated caspase-3 to the nucleus during butyric acid-induced apoptosis. *Biochem Biophys Res Commun* 1999;**260**:**3** 775–80.
40 Wöhrl W, Häcker G. Extent and limitation of the control of nuclear apoptosis by DNA-fragmenting factor. *Biochem Biophys Res Commun* 1999;**254**:**3** 552–8.
41 Merritt AJ, Potten CS, Watson AJ, *et al*. Differential expression of bcl-2 in intestinal epithelia. Correlation with attenuation of apoptosis in colonic crypts and the incidence of colonic neoplasia. *J Cell Sci* 1995;**108**:2261–71.